Climate
of the Past
Discussions

Burning-derived vanillic acid in an Arctic ice core from Tunu, Northeastern Greenland

Mackenzie M. Grieman[1], Murat Aydin[1], Joseph R. McConnell[2], and Eric S. Saltzman[1]

[1]Department of Earth System Science, University of California, Irvine, Irvine, California, 92697-3100, USA
[2]Division of Hydrologic Sciences, Desert Research Institute, Reno, Nevada, USA

Correspondence to: Mackenzie M. Grieman (mgrieman@uci.edu)

Abstract. In this study, vanillic acid was measured in the Tunu ice core from northeastern Greenland in samples covering the past 1700 years. Vanillic acid is an aerosol-borne aromatic methoxy acid, produced by the combustion of lignin during biomass burning. Air mass trajectory analysis indicates that North American boreal forests are likely the major source region for biomass burning aerosols deposited to the ice core site. Vanillic acid levels in the Tunu ice core range from <0.005-0.08 ppb.

5   Tunu vanillic acid exhibits centennial-scale variability in preindustrial ice, with elevated levels during the warm climates of the Roman Warm Period and Medieval Climate Anomaly, and lower levels during the cooler climates of the Late Antiquity Little Ice Age and the Little Ice Age. Analysis using a peak detection method revealed a positive correlation between vanillic acid in the Tunu ice core and both ammonium and black carbon in the north Greenland NEEM ice core. This is encouraging evidence that a consistent pattern of centennial-scale variability in North American high latitude fire may be recorded by various fire

10   proxies in Greenland ice.

1   Introduction

Proxy records of biomass burning are important for understanding the relationship between climate variability and fire on long time scales. A diverse range of paleoproxies have been used to reconstruct biomass burning, including fire scars on tree rings, sedimentary charcoal records, ice core records of gases and aerosol-borne chemicals (Blarquez et al., 2014; Legrand

15   et al., 2016; Marlon et al., 2008, 2016; Power et al., 2008, 2013; Rubino et al., 2016). These records reflect a wide range of different aspects of fire location, frequency, distribution, and intensity. The proxies also integrate over a wide span of spatial and temporal scales. Despite these efforts, there is not yet a coherent global picture of historical variations in biomass burning and their relationship to climate over the past few millennia.

  Northern Hemisphere burning trends on millennial time scales have been developed using composites of terrestrial sedimen-

20   tary charcoal records (Marlon et al., 2008). These suggest that Northern Hemisphere burning declined during the Common Era, from about 1-1750 CE, then increased until 1870 CE. During the industrial period, burning rose from 1900-1950, declined from 1950-2000, and rose again after 2000 CE (Marlon et al., 2016). This composite record reflects conditions in Europe and North America, with few records from northern Asia. Greenland ice core ammonium, black carbon, and levoglucosan provide evidence for elevated North American burning prior to 500 CE and from 1000-1200 CE, although these records are not en-

tirely consistent with each other (Chýlek et al., 1995; Legrand et al., 1992, 2016; McConnell et al., 2007; Rubino et al., 2016; Zennaro et al., 2014).

Aromatic acids in ice cores have also been used as ice core proxies for regional variability in biomass burning (Grieman et al., 2017, 2018, in review). These compounds are produced from the pyrolysis of lignin and they retain the basic structure of

5 the lignin backbone (Hedges and Mann, 1979; Hedges and Parker, 1976; Opsahl and Benner, 1995; Oros and Simoneit, 2001a, b; Simoneit, 2002; Vanholme et al., 2010; Akagi et al., 2011; Legrand et al., 2016). These compounds have been extensively studied in laboratory burning studies and atmospheric aerosols (Iinuma et al., 2007; Oros and Simoneit, 2001a; Oros et al., 2006; Otto et al., 2006; Rogge et al., 1998; Simoneit et al., 1999). Until recently, relatively few measurements of these types of compounds have been made on ice cores. Recent studies include measurements of vanillic and p-hydroxybenzoic acid on

10 cores from Greenland, Switzerland, the Kamchatka Peninsula, and Svalbard (Kawamura et al., 2012; McConnell et al., 2007; Müller-Tautges et al., 2016). The first continuous, millennial time scale ice core records of VA and p-HBA from Siberia and Svalbard have recently been published (Grieman et al., 2017, 2018, in review).

In this study, VA was analyzed in an ice core from the Tunu region in Northeastern Greenland (Fig. 1). The ice core samples range in age over the past 1700 years (268-2013 CE) and this study presents the first continuous millennial time scale ice core

15 record of VA from Greenland. The Tunu record is compared to previous records of VA from Siberian and Svalbard ice cores, to sedimentary charcoal records from likely source regions, and to patterns of historical climate change.

2 Methods

2.1 Ice core dating and sample collection

The Tunu ice core was drilled in 2013 to a depth of 212 m (Fig. 1; 78.04°N, 33.88°W, 2,000 m above sea level). The mean

20 annual temperature at the Tunu-N weather station is -27.5°C (78.02°N, 33.99°W, 2,113 m above sea level; Steffen and Box, 2001). The ice core site has an average accumulation rate of 0.100 m water equivalent year^{-1} (Sigl et al., 2015). The Tunu ice core age scale is based on the annual layer counting of non-sea salt sulfur and sodium signals (Fig. S1; Mernild et al., 2015). The Tunu time scale agrees to within ±2 years with the Northwest Greenland NEEM (NEEM-2011-S1) ice core based on comparison of the ages of major volcanic events (Mernild et al., 2015; Sigl et al., 2013, 2015).

25 Samples for this study were obtained from melting of a 33 x 33 mm cross section of the core (McConnell et al., 2001; Sigl et al., 2015; Mernild et al., 2015). Samples of the melt stream were collected continuously via fraction collector. Each sample has a time resolution of roughly 2.5 years.

2.2 Ice core sample analysis and data processing

Vanillic acid (VA) and para-hydroxybenzoic acid (p-HBA) were analyzed by anion exchange chromatographic separation and

30 tandem mass spectrometric detection with electrospray ionization in negative ion mode (Grieman et al., 2017, 2018, in review). VA and p-HBA were detected at mass transitions of m/z 167→108 and m/z 137→93, respectively. Synthetic standards prepared

using reagent grade VA and p-HBA in milli-Q water were analysed in sequence with ice core samples. Detection limits for VA and p-HBA were 0.005 ppb and 0.034 ppb, defined as 3x the standard deviation of MilliQ water blanks (n = 58). 575 ice core samples from the Tunu ice core were analyzed in this study.

Tunu ice core VA ranges from below detection to 0.080 ppb, which is about 15x the detection limit (Fig. 2). The distribution of the measurements was skewed strongly towards lower concentrations, with VA levels below detection in 40% of the samples. The VA measurements below detection were replaced in the data set with a value of one half the detection limit, or 0.0025 ppb. The geometric mean VA level for the whole data set was $0.005^{+0.007}_{-0.003}$ ppb.

In analyzing the Tunu vanillic acid data set, a number of different methods were examined, including: 1) bin averaging of the log-transformed data (Grieman et al., 2015), 2) LOESS smoothing (Cleveland and Devlin, 1988), and 3) peak detection using singular spectrum analysis (Higuera et al., 2010; Fischer et al., 2015). The trends discussed here are robust in the sense that they are evident regardless of the data analysis method used. For example, similar patterns of centennial variability emerge from all of the methods (Fig. S2).

Although p-HBA is present in many samples, the levels are not reported due to interference at the m/z 137→93 mass transition eluting at nearly the same retention time (Fig. S3). This peak was present in most of the ice core samples, blanks, and standards. The presence of this peak in blanks and standards suggests that it is a contaminant introduced during sample handling or storage. This peak was not observed in previous analyses of p-HBA in other Arctic ice cores (Grieman et al., 2017, 2018, in review).

3 Results and Discussion

3.1 Tunu vanillic acid time series

Tunu vanillic acid (VA) levels do not exhibit a significant linear trend over the past 1700 years. They do exhibit pronounced variability on both millennial and centennial time scales (Fig. 2). This variability is observable in the raw data as multi-decadal to century-long periods in which all of the measurements were above the detection limit. The variability is more clearly shown in the 40-year bin averages of the log-transformed data (Fig. 3). There is a maximum early in the record (280-400 CE) during the Roman Warm Period (RWP; 550 BCE-350 CE) followed by a period of generally lower levels from 500-1000 CE. A second maximum occurred during the Medieval Climate Anomaly (MCA; 1080-1240 CE) followed by generally declining levels through the Little Ice Age (LIA) and into the twentieth century. There is shorter-term (decadal or multi-decadal) variability throughout the record. A peak during the latter half of the twentieth century (1955-1985) stands out as the largest example of such variability in the record (Fig. 3, 4).

We also examined variability in the Tunu VA record by analyzing the frequency of occurrence of highly elevated VA levels. This "peak detection" approach has been used to extract fire proxy signals from sediment charcoal and ice core ammonium records (Higuera et al., 2010; Legrand et al., 2016; Fischer et al., 2015). To apply this method, we used singular spectrum analysis (SSA) to decompose the Tunu VA record into 30 principle components (PC's). The PC's were converted to reconstructed components (RC's). RC-1 contains most of the low frequency content of the Tunu VA record. This component shows similar

millennial-scale variability to the 40-year bin-averaged data, with elevated VA early in the record and around the MCA. It also emphasizes the decreasing trend from 1200-1900 CE and the increase during the 20th century (Fig. 5, top panel).

The higher frequency content of the VA record was reconstituted by summing RC's 2-30 (Fig. 5, middle panel). Individual peaks in the reconstituted record were detected as samples with VA levels exceeding a specified threshold. The threshold was

5 defined as a percentile of the reconstituted data and peak frequency (peaks year^{-1}) computed in a moving 40-year window. Peak thresholds of 65th, 70th, and 75th percentiles were used. The results are insensitive to the choice of threshold in this range (Fig. 5, lower panel). The peak detection algorithm shows strong centennial scale variability, in general agreement with the 40-year bin averaging. Clearly these are robust features of the Tunu VA record. The amplitudes of the centennial scale features are relatively constant until the onset of the Little Ice Age, after which they appear to decline. At face value, the peak

10 detection algorithm suggests that these centennial scale changes in Tunu VA involved not only variations in the abundance of VA, but also changes in the frequency large fire events. In theory, comparing peak detection and bin-averaging signals could differentiate between biomass burning aerosols from distant fiers that might be well-mixed throughout the Arctic atmosphere, as compared to large episodic inputs from major fire plumes in the immediate source regions impacting the site.

3.2 Relationship between Tunu vanillic acid levels and accumulation rate

15 Interpretation of ice core vanillic acid levels in terms of atmospheric aerosol concentrations or fluxes, requires consideration of the processes by which aerosols are incorporated into the polar ice sheet. The concentrations of ions in polar ice cores likely reflect changes in the composition and abundance of the overlying aerosols, but may also be influenced by depositional and post-depositional processes that affect the air/snow transfer function (Grannas et al., 2007). We examined the relationship between VA and snow accumulation rate in order to assess the influence of variations in local conditions on Tunu ice core

20 VA levels. VA flux was computed as the product of accumulation rate and VA concentration ($F = C_{ice} \, A_{H_2O} \, \rho_{ice}$). VA flux exhibits the same major features observed in the concentration record, indicating that the variations in VA likely reflect changes in atmospheric composition and are not caused primarily by changes in snow accumulation (Fig. 6). Excluding the 20th century, there is a positive correlation between VA flux and accumulation rate (r^2=0.27, $p < 0.001$) with slope of 0.011 ± 0.001 x 10^{-9} kg m^{-2} yr^{-1} VA / kg m^{-2} yr^{-1} water flux (Fig. 7). This positive relationship is typical of ice core impurities, and may be

25 interpreted in the context of a simple model of dry/wet deposition, such as:

$$F_{total} = F_{dry} + F_{wet}$$

$$= C_{air} \, v_d + C_{air} R_{scav} P_{H_2O},$$

where C_{air} is the concentration of VA in the atmosphere, V_d is a dry deposition velocity for the VA-containing aerosols, $R_s cav$

30 is the wet deposition scavenging ratio, and P_{H_2O} is the snow precipitation rate (Saltzman et al., 1997).

For a chemically stable, non-volatile species with variations in both atmospheric concentration and snow precipitation (that are not highly correlated), one would expect to observe: 1) a positive correlation between the depositional flux and water accumulation, and 2) a positive y-intercept reflecting the dry deposition component. A negative intercept could be interpreted as evidence of re-volatilization of VA from the snowpack, but the magnitude of this effect is evidently small.

During the 20th century, there is little change in accumulation rate associated with the very large increase in VA. This confirms that the 20th century increase is likely a real atmospheric feature and not an artifact related to local depositional conditions. If re-volatilization does occur after deposition, one would expect that loss of methoxy aromatic acids may increase with increased acidity. In this record, the opposite appears to be the case. Elevated levels of VA generally coincide with elevated

5   levels of acidity, sulfate, and, to a lesser degree, nitrate during the 20th century (Fig. S4; S5). Increased acidity therefore does not appear to have induced significant loss of vanillic acid from the Tunu ice core.

3.3 Potential source regions for Tunu vanillic acid

Air mass back trajectory studies indicate that North America is the major source region for aerosols transported to the central Greenland ice sheet (Kahl et al., 1997). Here we examine transport from potential biomass burning source regions to

10   the Tunu ice core site (78°N, 34°W) during the boreal burning season. 10-day air mass back trajectories were run from the Tunu ice core site at 12:00 AM and 12:00 PM local time (UTC-2 hours) beginning 100 m above ground level. Back trajectories were computed each day for spring (March 1-May 31), summer (June 8-August 31), and fall (September 1-November 30). The HYSPLIT model was used to compute the trajectories using NCEP/NCAR meteorological data for the ten-year period (2006-2015) (Kalnay et al., 1996; Draxler et al., 1999; Stein et al., 2015). Possible source regions were par-

15   titioned into ecofloristic zones in North America, Europe (defined as west of 42°E), and Siberia (defined as east of 42°E). Food and Agriculture Organization classifications were used to define ecofloristic zones in each of these regions (Fig. S6; http://cdiac.ornl.gov/epubs/ndp/global_carbon/carbon_documentation.html; Ruesch and Gibbs, 2008).

The back-trajectories confirm that aerosols reaching the Tunu site predominantly originated in North America. North American trajectories comprised 32%, 17%, and 37% of the total for spring, summer, and fall, respectively (Table 1; Fig. S7). The

20   most commonly transected North American ecofloristic zones were boreal tundra woodland and boreal coniferous forests. Trajectories from North American ecofloristic zones were more common in the fall and spring than in the summer. The percentages of trajectories from European and Siberian ecofloristic zones were all lower than 3% and 2%, respectively. These results do not preclude wildfire emissions from Europe or Siberia reaching the Tunu ice core site but suggest that the frequency of such events is much lower than that for North American events. This result is consistent with Kahl et al. (1997), an earlier study of

25   air mass transport to Summit, Greenland over a 40-year period (1946-1989).

3.4 Comparison to the NEEM Greenland ice core record of ammonium and black carbon

In order to develop confidence that ice core proxies of biomass burning are broadly representative of large-scale regional paleofire trends, it is important to demonstrate similar historical patterns from ice cores in the same geographic region and influenced by similar air mass trajectories. Here we compare Tunu VA with ammonium and black carbon measurements on

30   the NEEM ice core from North Greenland (Zennaro et al., 2014). Air mass trajectories indicate that the NEEM site should experience similar transport to Tunu, with eastern Canada as the major fire source region followed by western Canada (Legrand et al., 2016). We first compare Tunu VA and NEEM black carbon using the first principle component of a singular spectrum

analysis of each records (RC-1; Fig. 8). NEEM ammonium was not included in this analysis, as it is believed that long-term variations in ammonium levels reflect biogenic rather than pyrogenic emissions (Legrand et al., 2016; Fischer et al., 2015).

There are some similarities between Tunu VA and NEEM black carbon. Both records are low prior to the MCA and during the LIA and both records are elevated during the RWP and MCA. There are also notable differences. For example, vanillic

5 acid declines sharply into the Late Antique Little Ice Age (LALIA) around 450 CE, while black carbon and ammonium remain relatively high until 700 CE. Another difference is that black carbon reaches its LIA minima around 1750 and begins to rise thereafter. By contrast, VA continues its decline, reaching its minimum around 1900 CE. The divergence of these proxies during the industrial period is not surprising, as black carbon is emitted from fossil fuel combustion while VA is not. The divergence between VA and black carbon during the industrial period was previously observed in a shallow central Greenland ice core

10 (McConnell et al., 2007).

We next used the peak detection method described earlier in section 3.1 to examine the relationship of Tunu VA with NEEM ammonium and black carbon. A peak threshold of the 70th percentile was used for all records. For the data set as a whole, all three of the fire proxies are positively correlated with one another (p<0.001). Visual inspection of the results shows that the relationships between Tunu VA, NEEM ammonium, and NEEM black carbon are complex, with periods of both positive and

15 negative correlation. In order to better illustrate the relationships, we computed the correlation coefficient between the three pairs of proxies in a 200-year moving window (Fig. 8, lower panel). The results show a strong positive correlation for all the records from 650-1200 CE and a more variable and weaker relationship thereafter. This abrupt change in relationship occurs around the same time as a major change in North Atlantic climate discussed below (see section 3.6).

3.5 Comparison to charcoal records

20 We compared the Tunu ice core VA record to sedimentary charcoal records from North America. All charcoal records from Canada available in the Global Charcoal Database (106 records, 40°-80°N, 10°-160°W) were analyzed using the paleofire R package (http://gpwg.paleofire.org; Blarquez et al., 2014; Marlon et al., 2008). Regional Canadian charcoal records were normalized using the Box-Cox, mini-max, and z-score transformations for 200-2000 CE, and composited using 40-year bin averages.

25 The Canada charcoal record exhibits no linear trend and century time scale variability that is not significant at the 95% confidence interval (Fig. S8). We also examined composite records for a number of smaller regions within Canada in an effort to identify variability similar to that in Tunu VA (Fig. S9). These regions are also not significant at the 95% confidence interval. Only the records from western Canada (40°-80°N, 110°-180°W) show some similarity to the Tunu VA record with slight increases from 1000-1200 and 1300-1500. The qualitative similarities between the Tunu VA and western Canadian charcoal

30 record suggest that this may be a source region of the Greenland burning signals, but the correlation is not significant at the 95% confidence interval. The lack of significant correlation between charcoal records and Tunu VA can in part be due to uncertainties in chronologies as charcoal record chronologies generally have much larger uncertainties than ice cores.

3.6 Relationship to climate

Over the past two millennia, Northern Hemispheric climate has been modulated by several centennial-scale climate anomalies: the Roman Warm Period (550 BCE-350 CE; Wang et al., 2012), the Dark Ages Cold period (400-765 CE; Helama et al., 2017) or Late Antique Little Ice Age (536-660 CE; Büntgen et al., 2016), the Medieval Climate Anomaly (950-1250 CE; Mann

5 et al., 2009), and the Little Ice Age (1400-1700 CE; Mann et al., 2009). These climate anomalies appear to be reflected in the Tunu VA record, with elevated VA during the warm periods and lower levels during the colder periods (Fig. 9). The data suggest a positive correlation between North American fire and hemispheric mean temperature. This relationship could be due to climate-driven changes in temperature or precipitation on burning extent, frequency, or location, as well as to changes in atmospheric transport patterns.

10 Skinner et al. (2006) examined relationships between Canadian forest fire season severity and prior winter global sea surface temperature variations from 1953-1999. They found three principle modes of influence: 1) the global near-linear trend in SST (i.e. Southern ocean warming and Atlantic and North Central Pacific cooling) positively correlated with fire severity across most of Canada, 2) the modulation of Atlantic SST associated with the Atlantic Multidecadal Oscillation (AMO) or Variability (AMV), with high fire severity across most of Canada associated with Atlantic cooling, and 3) variations in Pacific

15 SST associated with PDO and ENSO, with high fire severity in western Canada and low severity over southern and eastern Canada associated with warm Pacific SST. Based on these results, one might speculate that externally forced climate variability due to orbital variations or volcanic eruptions might modulate Canada fire emissions via the global SST mode, while internal variability in the AMV and PDO modes might dominate on multi-decadal time scales (60-80 years). We examined several proxy reconstructions for these modes in order to test these relationships.

20 The PAGES Oceans 2K reconstruction shows a monotonic cooling trend for the global ocean over the past two millennia, with the exception of warming during the past century (McGregor et al., 2015). A notable exception to the trend is a period of warming in the Atlantic 1000-1300 CE during the MCA (Sicre et al., 2008, 2011, Fig. 9), while Pacific SST maintained its slow cooling trend. Proxy records indicate that both the AMV and the North Atlantic Oscillation were in the positive phase during this period, consistent with a warm Atlantic (Meeker and Mayewski, 2002; Trouet et al., 2009; Olsen et al., 2012; Wang

25 et al., 2017). Surprisingly, the observation of elevated Tunu VA during the warm MCA suggests a relationship of between North American fire and SST that is opposite in sign to inferred from analysis of the latter half of the 20th century by Skinner et al. (2006). That could indicate that different modes of variability influence North American fire on centennial and decadal time scales.

4 Conclusions

30 The Tunu ice core vanillic acid (VA) record is a new millennial time-scale record of burning emissions predominantly originating from the mid-high latitude forests of North America. At this stage, ice core VA should be regarded as a qualitative tracer. It is not known to what extent the signals reflect paleofire emissions, paleofire frequency, or changes in air mass transport and deposition. The correlation between Tunu VA, and NEEM ammonium and black carbon in the NEEM ice core is encouraging

evidence that a consistent pattern of centennial-scale variability in North American high latitude fire is recorded in Greenland ice, but further measurements on multiple ice cores will be needed to validate this conclusion. A clear link between the VA variability in Greenland ice and North American sedimentary charcoal is not evident, although a tentative connection to the Quebec region was noted. Further work on establishing these connections is needed. The apparent relationship between Tunu

5   VA and multi-century climate anomalies suggests that on long time scales, North American burning is positively correlated with Atlantic sea surface temperatures–a relationship that is not typical of the 20th century. The forcing and internal dynamics associated with late Holocene centennial scale climate variability remain a subject of debate and active research. Understanding those dynamics will be essential in order to unravel the fire-climate relationship.

5   Data availability

10   The data reported in this manuscript will be submitted to the NSF Artic Data Center (http://arcticdata.io/) before publication.

References

Akagi, S. K., Yokelson, R. J., Wiedinmyer, C., Alvarado, M. J., Reid, J. S., Karl, T., Crounse, J. D., and Wennberg, P. O.: Emission factors for open and domestic biomass burning for use in atmospheric models, Atmospheric Chemistry and Physics, 11, 4039–4072, doi:10.5194/acp-11-4039-2011, 2011.

5 Blarquez, O., Vannière, B., Marlon, J. R., Daniau, A.-L., Power, M. J., Brewer, S., and Bartlein, P. J.: Paleofire: An R package to analyse sedimentary charcoal records from the Global Charcoal Database to reconstruct past biomass burning, Computers and Geosciences, 72, 255 – 261, doi:10.1016/j.cageo.2014.07.020, 2014.

Büntgen, U., Myglan, V. S., Ljungqvist, F. C., McCormick, M., Di Cosmo, N., Sigl, M., Jungclaus, J., Wagner, S., Krusic, P. J., Esper, J., et al.: Cooling and societal change during the Late Antique Little Ice Age from 536 to around 660 AD, Nature Geoscience, 9, 231–236,

10 doi:10.1038/ngeo2652, 2016.

Chýlek, P., Johnson, B., Damiano, P. A., Taylor, K. C., and Clement, P.: Biomass burning record and black carbon in the GISP2 Ice Core, Geophysical Research Letters, 22, 89–92, doi:10.1029/94GL02841, 1995.

Cleveland, W. S. and Devlin, S. J.: Locally Weighted Regression: An Approach to Regression Analysis by Local Fitting, Journal of the American Statistical Association, 83, 596–610, doi:10.1080/01621459.1988.10478639, 1988.

15 Draxler, R. R., Stunder, B., Rolph, G., and Taylor, A.: HYSPLIT4 user's guide, NOAA Technical Memorandum ERL ARL, 230, 35, 1999.

Fischer, H., Schüpbach, S., Gfeller, G., Bigler, M., Röthlisberger, R., Erhardt, T., Stocker, T. F., Mulvaney, R., and Wolff, E. W.: Millennial changes in North American wildfire and soil activity over the last glacial cycle, Nature geoscience, 8, 723–727, doi:10.1038/ngeo2495, 2015.

Grannas, A. M., Jones, A. E., Dibb, J., Ammann, M., Anastasio, C., Beine, H. J., Bergin, M., Bottenheim, J., Boxe, C. S., Carver, G., Chen,

20 G., Crawford, J. H., Dominé, F., Frey, M. M., Guzmán, M. I., Heard, D. E., Helmig, D., Hoffmann, M. R., Honrath, R. E., Huey, L. G., Hutterli, M., Jacobi, H. W., Klán, P., Lefer, B., McConnell, J., Plane, J., Sander, R., Savarino, J., Shepson, P. B., Simpson, W. R., Sodeau, J. R., von Glasow, R., Weller, R., Wolff, E. W., and Zhu, T.: An overview of snow photochemistry: evidence, mechanisms and impacts, Atmospheric Chemistry and Physics, 7, 4329–4373, doi:10.5194/acp-7-4329-2007, 2007.

Grieman, M., Greaves, J., and Saltzman, E.: A method for analysis of vanillic acid in polar ice cores, Climate of the Past, 11, 227–232,

25 doi:10.5194/cp-11-227-2015, 2015.

Grieman, M. M., Aydin, M., Fritzsche, D., McConnell, J. R., Opel, T., Sigl, M., and Saltzman, E. S.: Aromatic acids in a Eurasian Arctic ice core: a 2600-year proxy record of biomass burning, Climate of the Past, 13, 395–410, doi:10.5194/cp-13-395-2017, 2017.

Hedges, J. I. and Mann, D. C.: The characterization of plant tissues by their lignin oxidation products, Geochimica et Cosmochimica Acta, 43, 1803–1807, doi:10.1016/0016-7037(79)90028-0, 1979.

30 Hedges, J. I. and Parker, P. L.: Land-derived organic matter in surface sediments from the Gulf of Mexico, Geochimica et Cosmochimica Acta, 40, 1019–1029, doi:10.1016/0016-7037(76)90044-2, 1976.

Helama, S., Jones, P. D., and Briffa, K. R.: Dark Ages Cold Period: A literature review and directions for future research, The Holocene, pp. 1–7, doi:10.1177/0959683617693898, 2017.

Higuera, P. E., Gavin, D. G., Bartlein, P. J., and Hallett, D. J.: Peak detection in sediment–charcoal records: impacts of alternative data

35 analysis methods on fire-history interpretations, International Journal of Wildland Fire, 19, 996–1014, doi:10.1071/WF09134, 2010.

Iinuma, Y., Brüggemann, E., Gnauk, T., Müller, K., Andreae, M. O., Helas, G., Parmar, R., and Herrmann, H.: Source characterization of biomass burning particles: The combustion of selected European conifers, African hardwood, savanna grass, and German and Indonesian peat, Journal of Geophysical Research: Atmospheres, 112, D08 209, doi:10.1029/2006JD007120, 2007.

Kahl, J. D. W., Martinez, D. A., Kuhns, H., Davidson, C. I., Jaffrezo, J.-L., and Harris, J. M.: Air mass trajectories to Summit, Greenland: A 44-year climatology and some episodic events, Journal of Geophysical Research: Oceans, 102, 26 861–26 875, doi:10.1029/97JC00296, 1997.

Kalnay, E., Kanamitsu, M., Kistler, R., Collins, W., Deaven, D., Gandin, L., Iredell, M., Saha, S., White, G., Woollen, J., Zhu, Y., Leetmaa, A., Reynolds, B., Chelliah, M., Ebisuzaki, W., Higgins, W., Janowiak, J., Mo, K., Ropelewski, C., Wang, J., Jenne, R., and Joseph, D.: The NCEP/NCAR 40-Year Reanalysis Project, Bulletin of the American Meteorological Society, 77, 437–471, 1996.

Kawamura, K., Izawa, Y., Mochida, M., and Shiraiwa, T.: Ice core records of biomass burning tracers (levoglucosan and dehydroabietic, vanillic and p-hydroxybenzoic acids) and total organic carbon for past 300 years in the Kamchatka Peninsula, Northeast Asia, Geochimica et Cosmochimica Acta, 99, doi:10.1016/j.gca.2012.08.006, 2012.

Legrand, M., De Angelis, M., Staffelbach, T., Neftel, A., and Stauffer, B.: Large perturbations of ammonium and organic acids content in the summit-Greenland Ice Core. Fingerprint from forest fires?, Geophysical Research Letters, 19, 473–475, doi:10.1029/91GL03121, 1992.

Legrand, M., McConnell, J., Fischer, H., Wolff, E. W., Preunkert, S., Arienzo, M., Chellman, N., Leuenberger, D., Maselli, O., Place, P., Sigl, M., Schüpbach, S., and Flannigan, M.: Boreal fire records in Northern Hemisphere ice cores: a review, Climate of the Past, 12, 2033–2059, doi:10.5194/cp-12-2033-2016, 2016.

Mann, M. E., Zhang, Z., Hughes, M. K., Bradley, R. S., Miller, S. K., Rutherford, S., and Ni, F.: Proxy-based reconstructions of hemispheric and global surface temperature variations over the past two millennia, Proceedings of the National Academy of Sciences, 105, 13 252–13 257, doi:10.1073/pnas.0805721105, 2008.

Mann, M. E., Zhang, Z., Rutherford, S., Bradley, R. S., Hughes, M. K., Shindell, D., Ammann, C., Faluvegi, G., and Ni, F.: Global Signatures and Dynamical Origins of the Little Ice Age and Medieval Climate Anomaly, Science, 326, 1256–1260, doi:10.1126/science.1177303, 2009.

Marlon, J. R., Bartlein, P. J., Carcaillet, C., Gavin, D. G., Harrison, S. P., Higuera, P. E., Joos, F., Power, M. J., and Prentice, I. C.: Climate and human influences on global biomass burning over the past two millennia, Nature Geosci, 1, 697–702, doi:10.1038/ngeo313, 2008.

Marlon, J. R., Kelly, R., Daniau, A.-L., Vannière, B., Power, M. J., Bartlein, P., Higuera, P., Blarquez, O., Brewer, S., Brücher, T., Feurdean, A., Romera, G. G., Iglesias, V., Maezumi, S. Y., Magi, B., Courtney Mustaphi, C. J., and Zhihai, T.: Reconstructions of biomass burning from sediment-charcoal records to improve data–model comparisons, Biogeosciences, 13, 3225–3244, doi:10.5194/bg-13-3225-2016, 2016.

McConnell, J. R., Lamorey, G. W., Lambert, S. W., and Taylor, K. C.: Continuous Ice-Core Chemical Analyses Using Inductively Coupled Plasma Mass Spectrometry, Environmental Science and Technology, 36, 7–11, 2001.

McConnell, J. R., Edwards, R., Kok, G. L., Flanner, M. G., Zender, C. S., Saltzman, E. S., Banta, J. R., Pasteris, D. R., Carter, M. M., and Kahl, J. D. W.: 20th-Century Industrial Black Carbon Emissions Altered Arctic Climate Forcing, Science, 317, 1381–1384, doi:10.1126/science.1144856, 2007.

McGregor, H. V., Evans, M. N., Goosse, H., Leduc, G., Martrat, B., Addison, J. A., Mortyn, P. G., Oppo, D. W., Seidenkrantz, M.-S., Sicre, M.-A., et al.: Robust global ocean cooling trend for the pre-industrial Common Era, Nature Geoscience, 8, 671–677, doi:10.1038/ngeo2510, 2015.

Meeker, L. D. and Mayewski, P. A.: A 1400-year high-resolution record of atmospheric circulation over the North Atlantic and Asia, The Holocene, 12, 257–266, doi:10.1191/0959683602hl542ft, 2002.

Mernild, S. H., Hanna, E., McConnell, J. R., Sigl, M., Beckerman, A. P., Yde, J. C., Cappelen, J., Malmros, J. K., and Steffen, K.: Greenland precipitation trends in a long-term instrumental climate context (1890–2012): evaluation of coastal and ice core records, International

5   Journal of Climatology, 35, 303–320, doi:10.1002/joc.3986, 2015.

Müller-Tautges, C., Eichler, A., Schwikowski, M., Pezzatti, G. B., Conedera, M., and Hoffmann, T.: Historic records of organic compounds from a high Alpine glacier: influences of biomass burning, anthropogenic emissions, and dust transport, Atmospheric Chemistry and Physics, 16, 1029–1043, doi:10.5194/acp-16-1029-2016, 2016.

Olsen, J., Anderson, N. J., and Knudsen, M. F.: Variability of the North Atlantic Oscillation over the past 5,200 years, Nature Geoscience, 5,

10   808–812, 2012.

Opsahl, S. and Benner, R.: Early diagenesis of vascular plant tissues: lignin and cutin decomposition and biogeochemical implications, Geochimica et Cosmochimica Acta, 59, 4889–4904, doi:10.1016/0016-7037(95)00348-7, 1995.

Oros, D. R. and Simoneit, B. R. T.: Identification and emission factors of molecular tracers in organic aerosols from biomass burning Part 1. Temperate climate conifers, Applied Geochemistry, 16, 1513–1544, doi:10.1016/s0883-2927(01)00021-x, 2001a.

15 Oros, D. R. and Simoneit, B. R. T.: Identification and emission factors of molecular tracers in organic aerosols from biomass burning Part 2. Deciduous trees, Applied Geochemistry, 16, 1545–1565, doi:10.1016/S0883-2927(01)00022-1, 2001b.

Oros, D. R., Abas, M. R. b., Omar, N. Y. M. J., Rahman, N. A., and Simoneit, B. R. T.: Identification and emission factors of molecular tracers in organic aerosols from biomass burning: Part 3. Grasses, Applied Geochemistry, 21, 919–940, doi:10.1016/j.apgeochem.2006.01.008, 2006.

20 Otto, A., Gondokusumo, R., and Simpson, M. J.: Characterization and quantification of biomarkers from biomass burning at a recent wildfire site in Northern Alberta, Canada, Applied Geochemistry, 21, 166 – 183, doi:10.1016/j.apgeochem.2005.09.007, 2006.

Power, M., Marlon, J., Ortiz, N., Bartlein, P., Harrison, S., Mayle, F., Ballouche, A., Bradshaw, R., Carcaillet, C., Cordova, C., Mooney, S., Moreno, P., Prentice, I., Thonicke, K., Tinner, W., Whitlock, C., Zhang, Y., Zhao, Y., Ali, A., Anderson, R., Beer, R., Behling, H., Briles, C., Brown, K., Brunelle, A., Bush, M., Camill, P., Chu, G., Clark, J., Colombaroli, D., Connor, S., Daniau, A. L., Daniels, M., Dodson, J.,

25 Doughty, E., Edwards, M., Finsinger, W., Foster, D., Frechette, J., Gaillard, M. J., Gavin, D., Gobet, E., Haberle, S., Hallett, D., Higuera, P., Hope, G., Horn, S., Inoue, J., Kaltenrieder, P., Kennedy, L., Kong, Z., Larsen, C., Long, C., Lynch, J., Lynch, E., McGlone, M., Meeks, S., Mensing, S., Meyer, G., Minckley, T., Mohr, J., Nelson, D., New, J., Newnham, R., Noti, R., Oswald, W., Pierce, J., Richard, P., Rowe, C., Sanchez Goñi, M., Shuman, B., Takahara, H., Toney, J., Turney, C., Urrego-Sanchez, D., Umbanhowar, C., Vandergoes, M., Vanniere, B., Vescovi, E., Walsh, M., Wang, X., Williams, N., Wilmshurst, J., and Zhang, J.: Changes in fire regimes since the Last Glacial Maximum: an

30 assessment based on a global synthesis and analysis of charcoal data, Climate Dynamics, 30, 887–907, doi:10.1007/s00382-007-0334-x, 2008.

Power, M., Mayle, F., Bartlein, P., Marlon, J., Anderson, R., Behling, H., Brown, K., Carcaillet, C., Colombaroli, D., Gavin, D., Hallett, D., Horn, S., Kennedy, L., Lane, C., Long, C., Moreno, P., Paitre, C., Robinson, G., Taylor, Z., and Walsh, M.: Climatic control of the biomass-burning decline in the Americas after AD 1500, The Holocene, 23, 3–13, doi:10.1177/0959683612450196, 2013.

35 Rogge, W. F., Hildemann, L. M., Mazurek, M. A., Cass, G. R., and Simoneit, B. R.: Sources of Fine Organic Aerosol. 9. Pine, Oak, and Synthetic Log Combustion in Residential Fireplaces, Environmental Science & Technology, 32, 13–22, doi:10.1021/es960930b, 1998.

Rubino, M., D'Onofrio, A., Seki, O., and Bendle, J. A.: Ice-core records of biomass burning, The Anthropocene Review, 3, 140–162, doi:10.1177/2053019615605117, 2016.

Ruesch, A. and Gibbs, H. K.: New IPCC Tier-1 global biomass carbon map for the year 2000, Carbon Dioxide Information Analysis Center, Oak Ridge National Laboratory, 2008.

Saltzman, E. S., Whung, P.-Y., and Mayewski, P. A.: Methanesulfonate in the Greenland Ice Sheet Project 2 Ice Core, Journal of Geophysical Research: Oceans, 102, 26 649–26 657, doi:10.1029/97JC01377, 1997.

5   Sicre, M.-A., Jacob, J., Ezat, U., Rousse, S., Kissel, C., Yiou, P., Eiríksson, J., Knudsen, K. L., Jansen, E., and Turon, J.-L.: Decadal variability of sea surface temperatures off North Iceland over the last 2000 years, Earth and Planetary Science Letters, 268, 137 – 142, doi:http://dx.doi.org/10.1016/j.epsl.2008.01.011, 2008.

Sicre, M.-A., Hall, I. R., Mignot, J., Khodri, M., Ezat, U., Truong, M.-X., Eiríksson, J., and Knudsen, K.-L.: Sea surface temperature variability in the subpolar Atlantic over the last two millennia, Paleoceanography, 26, PA4218, doi:10.1029/2011PA002169, 2011.

10   Sigl, M., McConnell, J. R., Layman, L., Maselli, O., McGwire, K., Pasteris, D., Dahl-Jensen, D., Steffensen, J. P., Vinther, B., Edwards, R., Mulvaney, R., and Kipfstuhl, S.: A new bipolar ice core record of volcanism from WAIS Divide and NEEM and implications for climate forcing of the last 2000 years, Journal of Geophysical Research: Atmospheres, 118, 1151–1169, doi:10.1029/2012JD018603, 2013.

Sigl, M., Winstrup, M., McConnell, J., Welten, K., Plunkett, G., Ludlow, F., Büntgen, U., Caffee, M., Chellman, N., Dahl-Jensen, D., et al.: Timing and climate forcing of volcanic eruptions for the past 2,500 years, Nature, 523, 543–549, doi:10.1038/nature14565, 2015.

15   Simoneit, B., Schauer, J., Nolte, C., Oros, D., Elias, V., Fraser, M., Rogge, W., and Cass, G.: Levoglucosan, a tracer for cellulose in biomass burning and atmospheric particles, Atmospheric Environment, 33, 173–182, doi:10.1016/S1352-2310(98)00145-9, 1999.

Simoneit, B. R. T.: Biomass burning - A review of organic tracers for smoke from incomplete combustion, Applied Geochemistry, 17, 129–162, doi:10.1016/S0883-2927(01)00061-0, 2002.

Skinner, W. R., Shabbar, A., Flannigan, M. D., and Logan, K.: Large forest fires in Canada and the relationship to global sea surface

20   temperatures, Journal of Geophysical Research: Atmospheres, 111, D14 106, doi:10.1029/2005JD006738, 2006.

Steffen, K. and Box, J.: Surface climatology of the Greenland ice sheet: Greenland Climate Network 1995–1999, Journal of Geophysical Research: Atmospheres, 106, 33 951–33 964, 2001.

Stein, A., Draxler, R., Rolph, G., Stunder, B., Cohen, M., and Ngan, F.: NOAA's HYSPLIT atmospheric transport and dispersion modeling system, Bulletin of the American Meteorological Society, 96, 2059–2077, doi:10.1175/BAMS-D-14-00110.1, 2015.

25   Trouet, V., Esper, J., Graham, N. E., Baker, A., Scourse, J. D., and Frank, D. C.: Persistent Positive North Atlantic Oscillation Mode Dominated the Medieval Climate Anomaly, Science, 324, 78–80, doi:10.1126/science.1166349, 2009.

Vanholme, R., Demedts, B., Morreel, K., Ralph, J., and Boerjan, W.: Lignin biosynthesis and structure, Plant Physiology, 153, 895–905, doi:10.1104/pp.110.155119, 2010.

Wang, J., Yang, B., Ljungqvist, F. C., Luterbacher, J., Osborn, T. J., Briffa, K. R., and Zorita, E.: Internal and external forcing of multidecadal

30   Atlantic climate variability over the past 1,200 years, Nature Geoscience, pp. 1–7, doi:10.1038/ngeo2962, 2017.

Wang, T., Surge, D., and Mithen, S.: Seasonal temperature variability of the Neoglacial (3300–2500BP) and Roman Warm Period (2500–1600BP) reconstructed from oxygen isotope ratios of limpet shells (Patella vulgata), Northwest Scotland, Palaeogeography, Palaeoclimatology, Palaeoecology, 317, 104 – 113, doi:10.1016/j.palaeo.2011.12.016, 2012.

Zennaro, P., Kehrwald, N., McConnell, J. R., Schüpbach, S., Maselli, O. J., Marlon, J., Vallelonga, P., Leuenberger, D., Zangrando, R.,

35   Spolaor, A., Borrotti, M., Barbaro, E., Gambaro, A., and Barbante, C.: Fire in ice: two millennia of boreal forest fire history from the Greenland NEEM ice core, Climate of the Past, 10, 1905–1924, doi:10.5194/cp-10-1905-2014, 2014.

Table 1. Percentages of air mass back trajectories crossing-over or reaching various geographic regions and ecofloristic zones beginning at the Tunu drilling site (% rounded to nearest integer). Ecofloristic zones are defined using Food and Agriculture Organization classifications (Fig. S2; http://cdiac.ornl.gov/epubs/ndp/global_carbon/carbon_documentation.html; Ruesch and Gibbs, 2008).

Geographic region	Ecofloristic zone	Season		
		Spring	Summer	Fall
North America	boreal tundra woodland	10	3	14
	boreal coniferous forests	6	2	8
	other	16	12	15
	total	32	17	37
Europe	total	4	2	4
Siberia	total	3	1	4
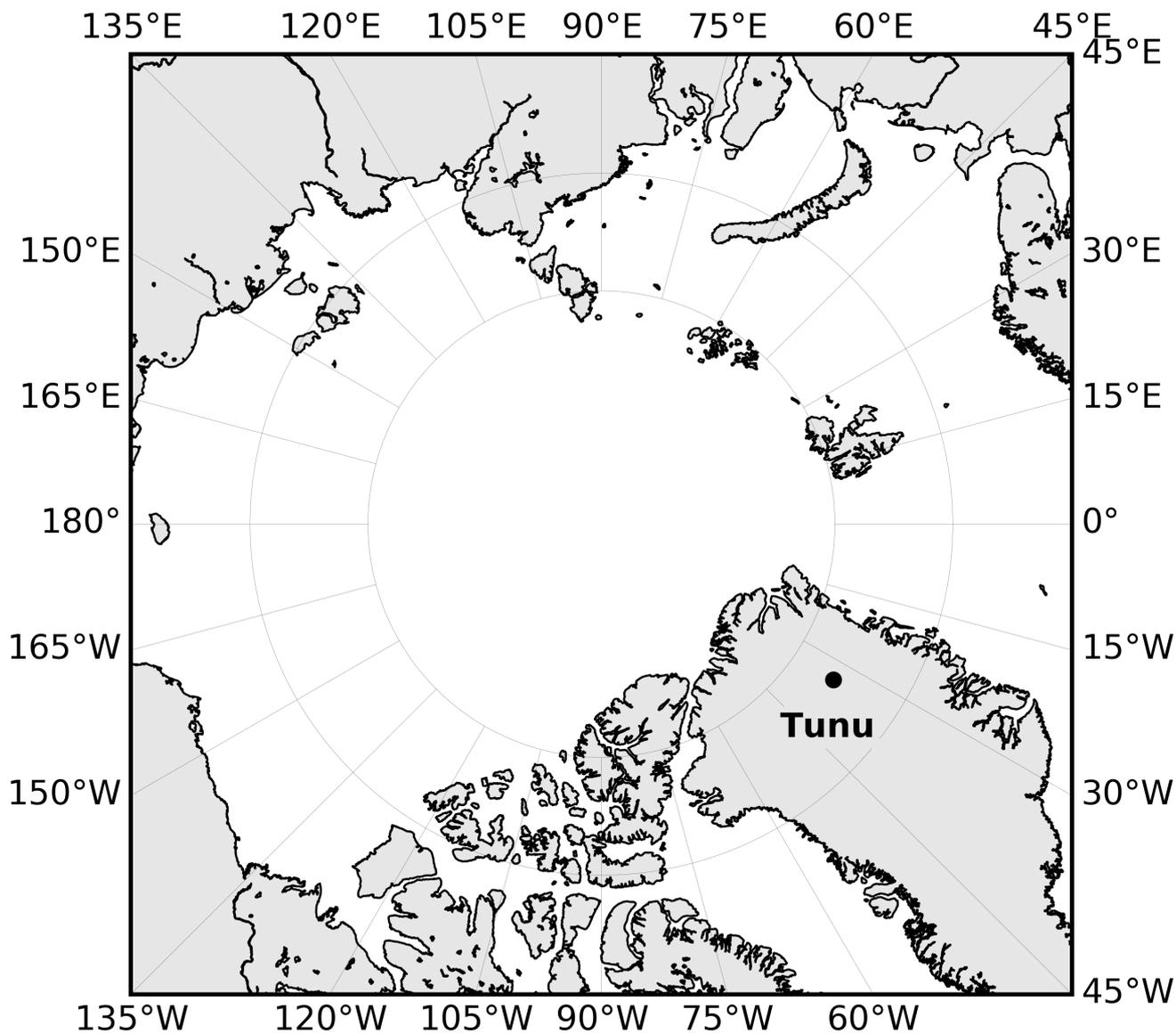
Figure 1. Tunu ice core drilling site (78.04°N, 33.88°W).
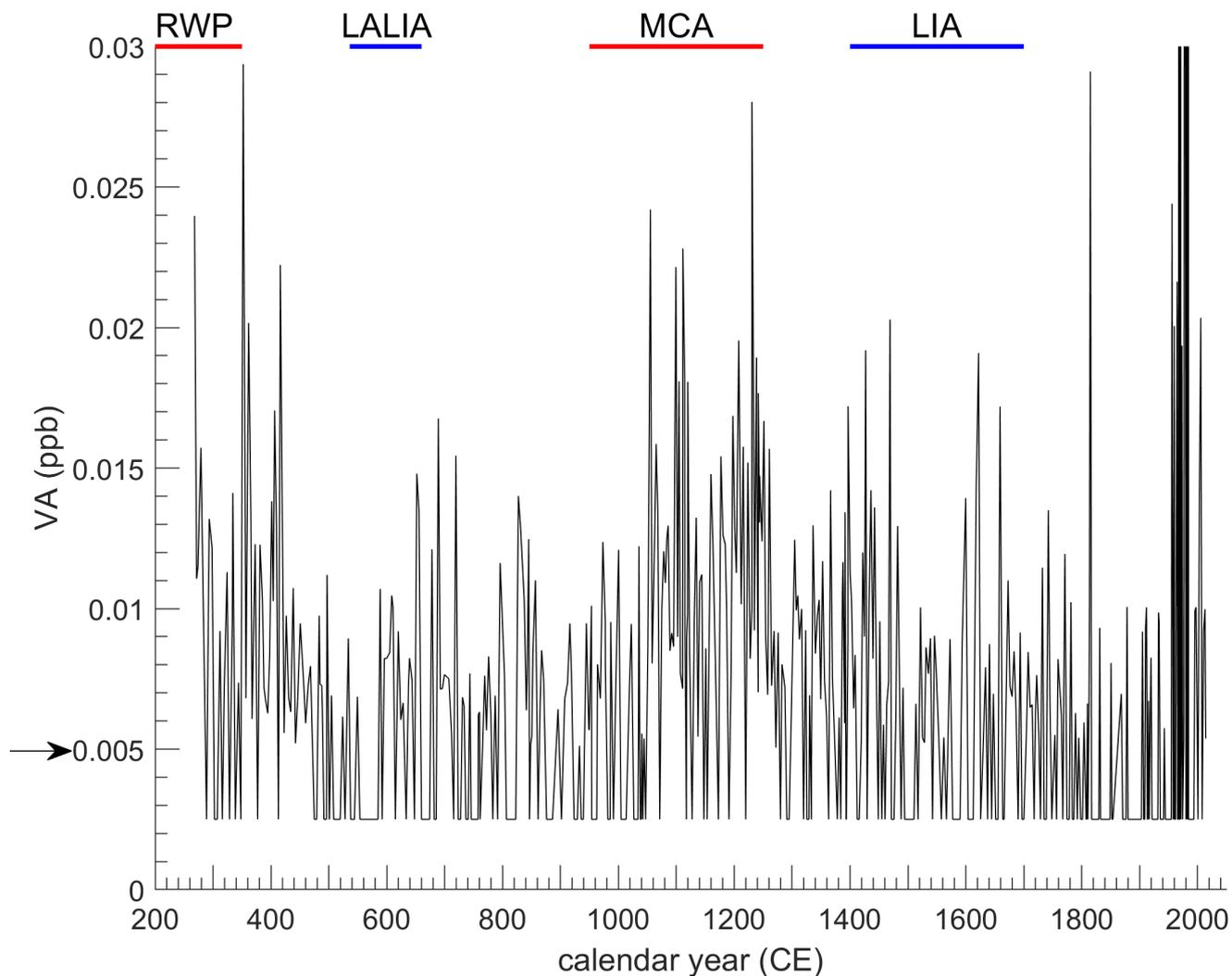
Figure 2. Tunu ice core vanillic acid (VA) record. The horizontal lines show the Roman Warm Period (RWP), Late Antique Little Ice Age (LALIA), Medieval Climate Anomaly (MCA), and the Little Ice Age (LIA) (Büntgen et al., 2016; Mann et al., 2009; Wang et al., 2012). The arrow indicates the limit of detection. All data below the limit of detection is treated as half of the limit of detection. Six measurements above 0.03 ppb not shown in this figure are shown in Fig. 4.
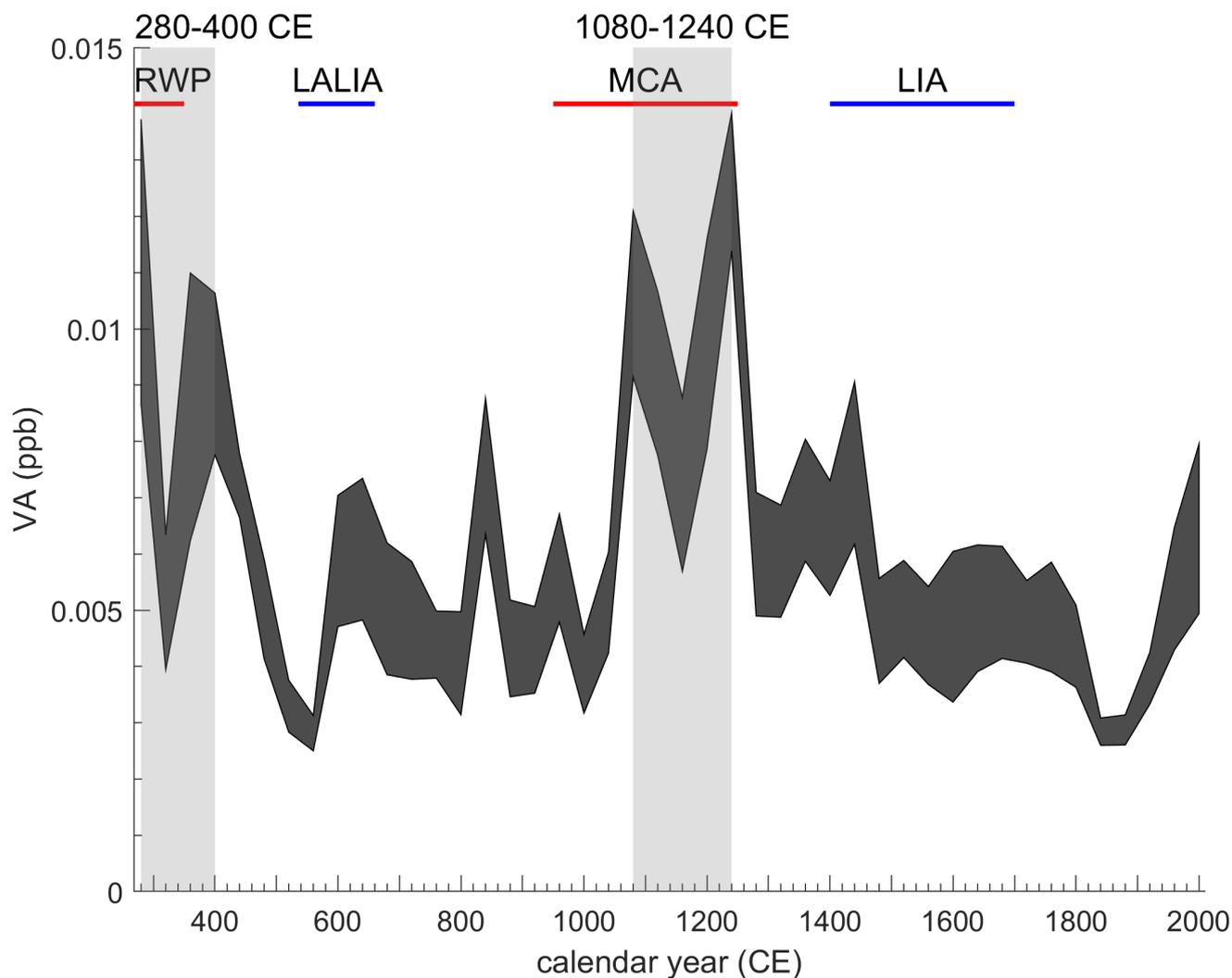
Figure 3. Tunu ice core vanillic acid (VA) record. The gray filled lines are ± 1 standard errors of the 40-year bin averages of the data. The horizontal lines show the Roman Warm Period (RWP), Late Antique Little Ice Age (LALIA), Medieval Climate Anomaly (MCA), and the Little Ice Age (LIA) (Büntgen et al., 2016; Mann et al., 2009; Wang et al., 2012). Light gray shaded areas are elevated periods in the record.
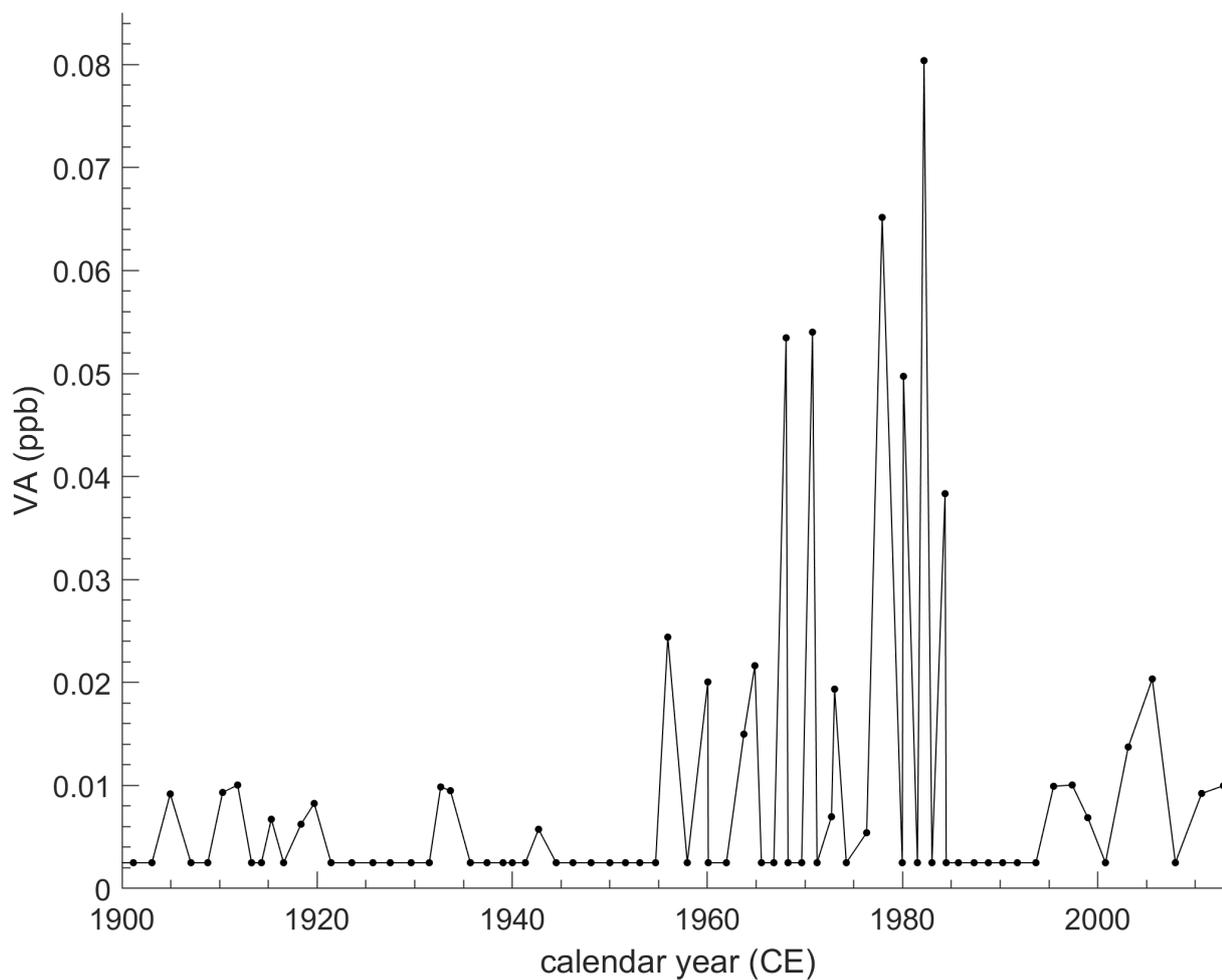
Figure 4. 20th century Tunu ice core vanillic acid (VA) record.
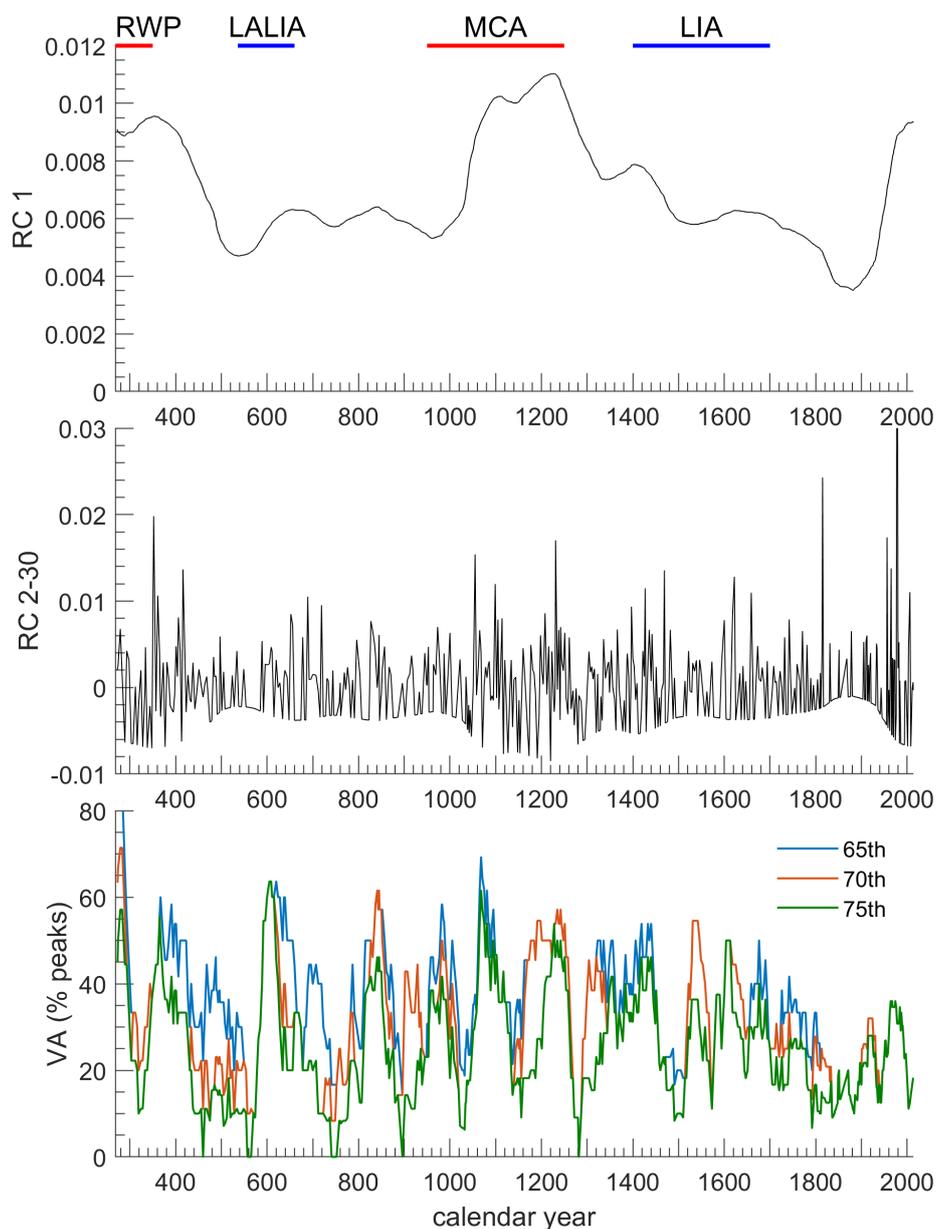
Figure 5. Tunu ice core vanillic acid analyzed by singular spectrum analysis (SSA) and peak detection showing millennial and centennial scale variability. 1) Low frequency variability in Tunu vanillic acid reconstructed using component 1 of the SSA, 2) higher frequency variability in Tunu vanillic acid reconstructed using SSA components 2-30, excluding component 1, 3) Peaks detected in the higher frequency Tunu vanillic reconstruction (components 2-30), shown as the fraction of ice core samples exceeding a peak threshold (65th, 70th, or 75th percentile) in a 40-year running window. The horizontal lines at top show the Roman Warm Period (RWP), Late Antique Little Ice Age (LALIA), Medieval Climate Anomaly (MCA), and the Little Ice Age (LIA) (Büntgen et al., 2016; Mann et al., 2009; Wang et al., 2012).

18

Climate
of the Past
Discussions
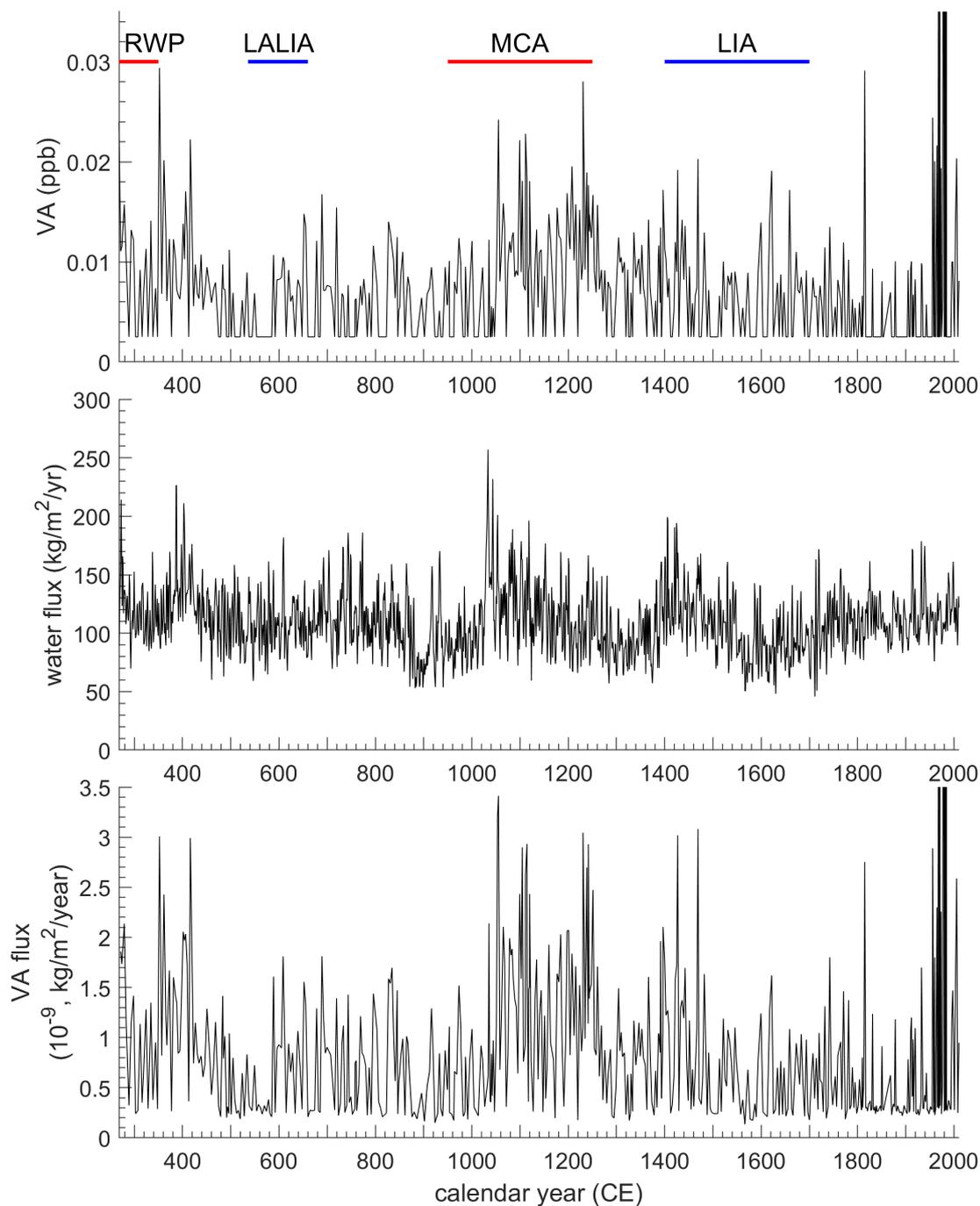
Figure 6. Tunu ice core vanillic acid concentration (top), water accumulation flux (middle), and vanillic acid depositional flux (bottom) computed as the product of vanillic acid concentration and water accumulation flux. The horizontal lines at top show the Roman Warm Period (RWP), Late Antique Little Ice Age (LALIA), Medieval Climate Anomaly (MCA), and the Little Ice Age (LIA) (Büntgen et al., 2016; Mann et al., 2009; Wang et al., 2012).

Climate
of the Past

Discussions

Open Access
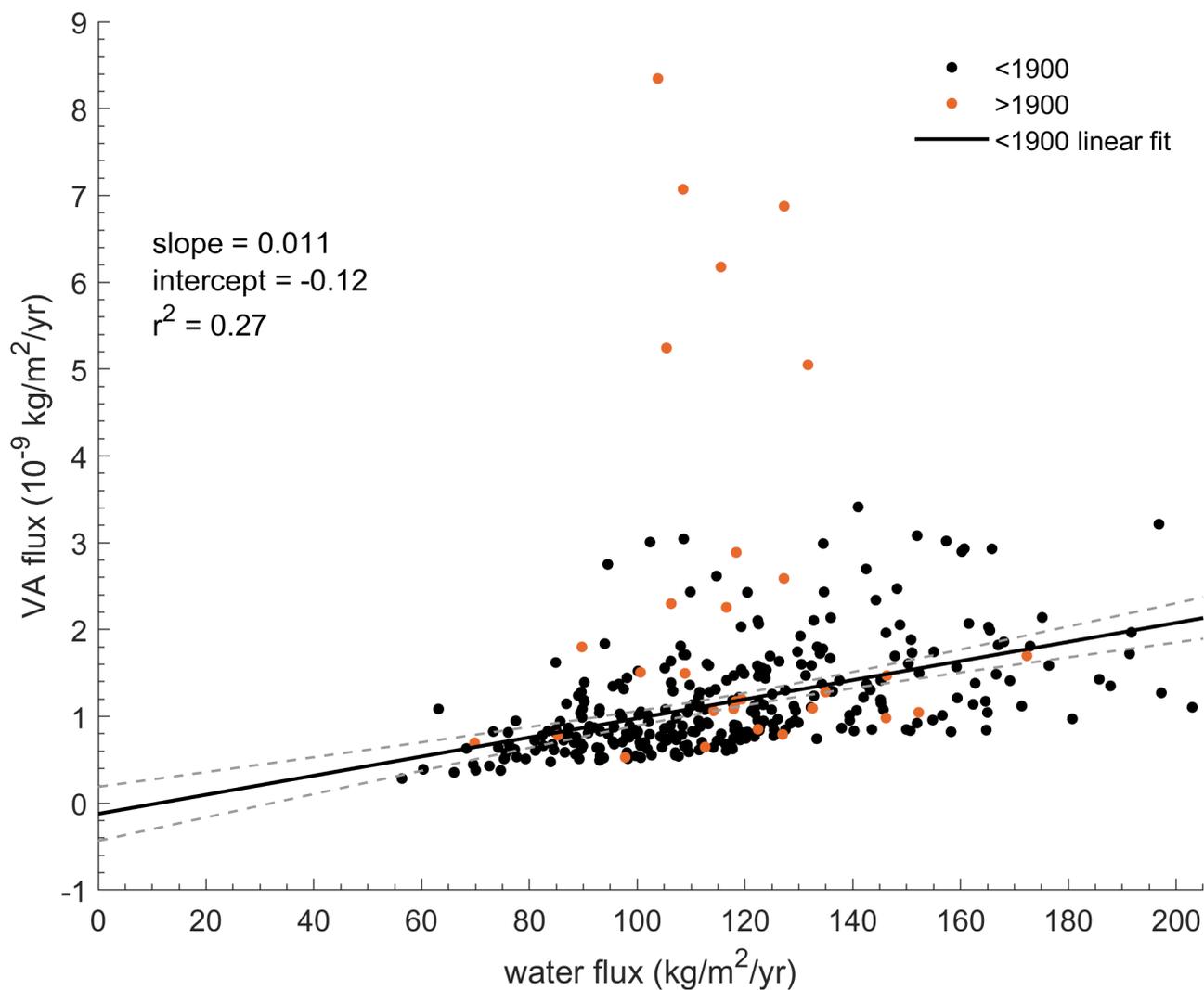
Figure 7. Relationship between Tunu vanillic acid depositional flux and water accumulation flux with linear regression to samples with ages older than 1900 CE (black points and line). Data younger than 1900 are shown in orange. Gray dashed lines show the uncertainty in the slope and intercept. Data below the limit of detection are not included.
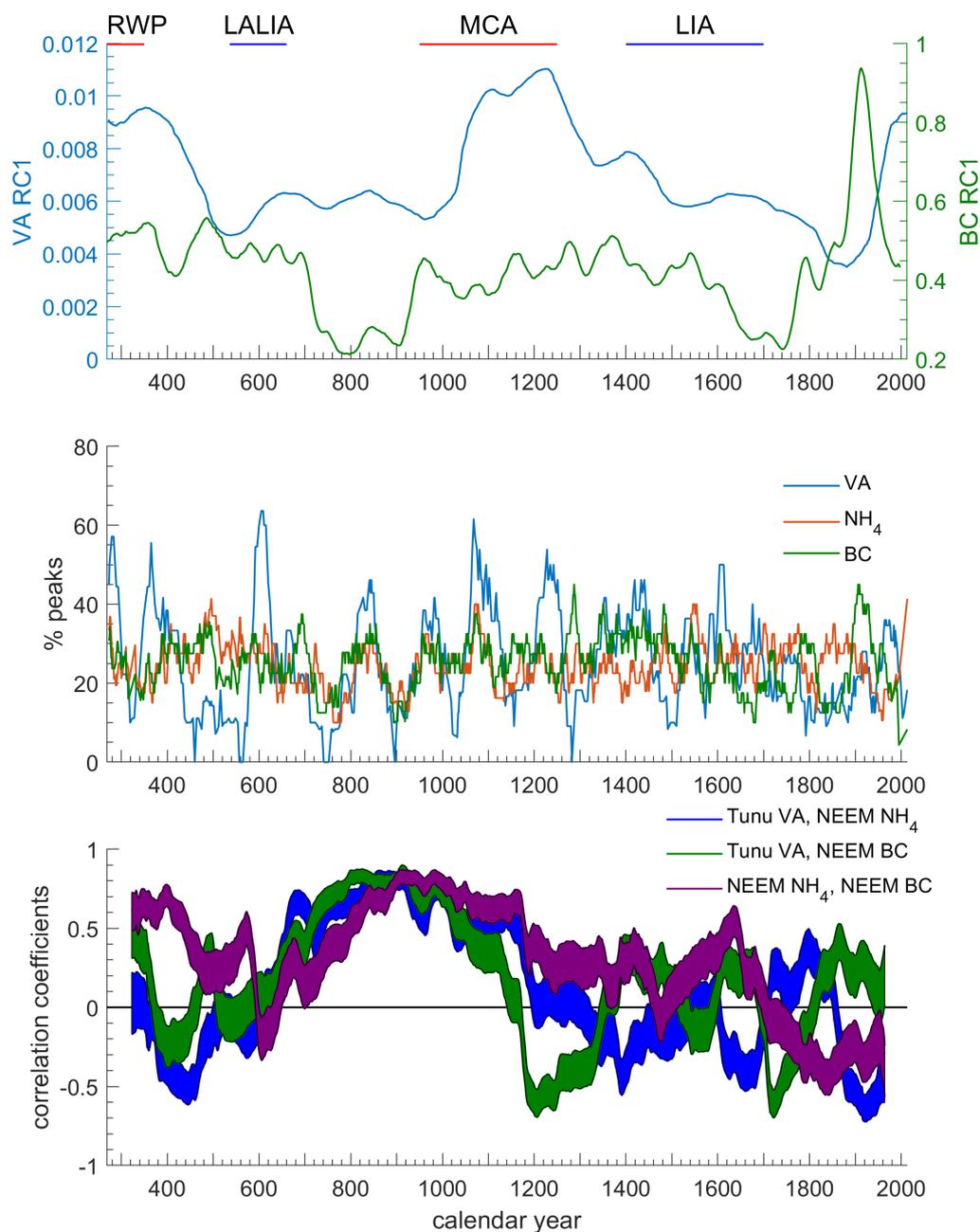
Figure 8. Relationships between biomass burning proxies in two north Greenland ice cores for the past 1700 years: Tunu ice core vanillic acid (VA), NEEM ammonium (NH_4) and NEEM black carbon (BC). 1) First component from the singular spectrum analysis of the three ice core signals (PC-1), 2) Frequency of peaks in the ice core signals reconstructed using singular spectrum components 2-30 and peak threshold of 75th percentile, smoothed with a 40-year running window, 3) 95% confidence intervals of correlation coefficients for the ice core peak frequencies using a 200-year running window ($p<0.001$). The horizontal lines at top show the Roman Warm Period (RWP), Late Antique Little Ice Age (LALIA), Medieval Climate Anomaly (MCA), and the Little Ice Age (LIA) (Büntgen et al., 2016; Mann et al., 2009; Wang et al., 2012).
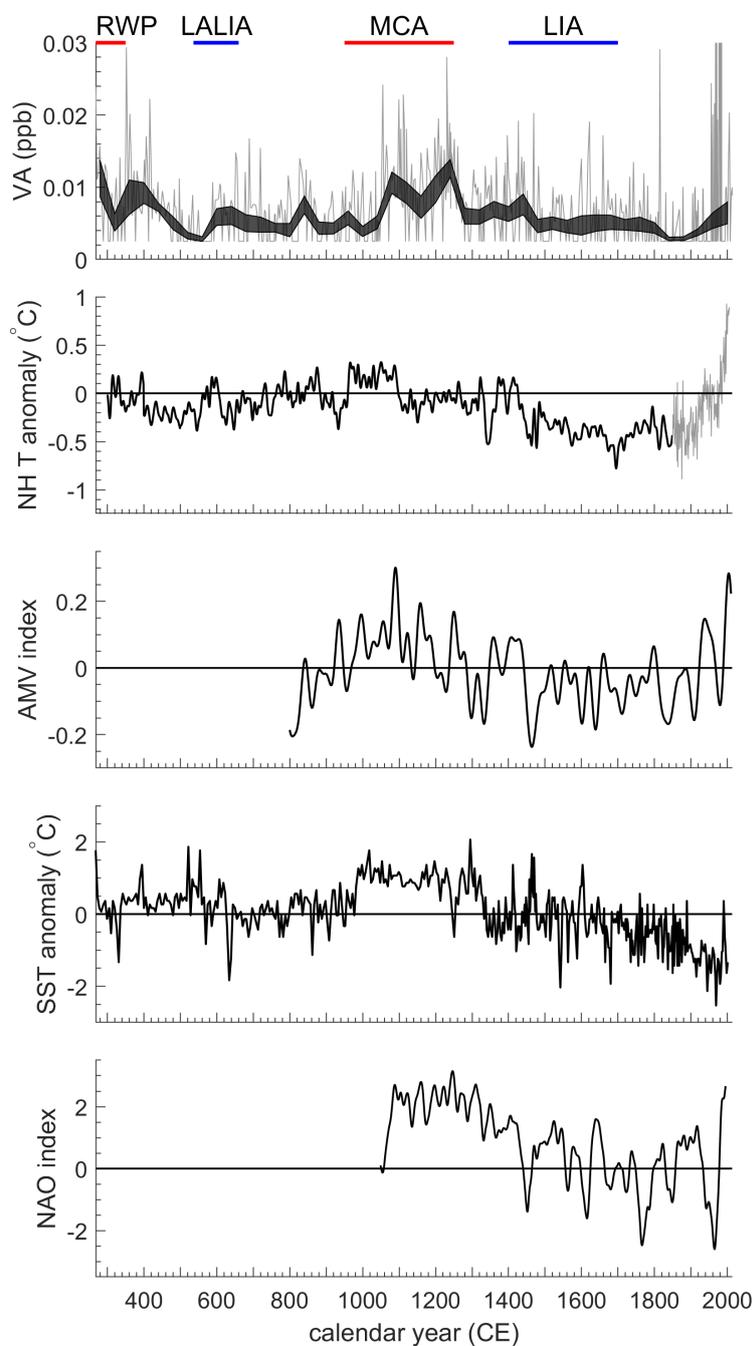
Figure 9. Comparison between Tunu vanillic acid (VA) and climate records. From top: Tunu VA, the gray filled lines are ± 1 standards errors of the 40-year bin averages of the data; Northern hemisphere land temperature anomaly composite before 1850 (EIV method; black line) and after 1850 (CRU instrumental record; www.cru.uea.ac.uk/cru/data/temperature; gray line) (Mann et al., 2008); 30-year low-pass filtered Atlantic multidecadal variability (AMV) (Wang et al., 2017); North Atlantic alkenone sea surface temperature (SST) anomaly based on MD99-2275 sediment (Sicre et al., 2011); and North Atlantic Oscillation (NAO) index reconstruction (Trouet et al., 2009).